

# Neuromimetic motion indicator for visual perception

Claudio CASTELLANOS SÁNCHEZ \*

Laboratory of Information Technologies - Centre for Research and Advanced Studies  
Km 6 carretera Cd. Victoria-Monterrey, 87276 Victoria, Tamaulipas - MEXICO.

**Abstract.** This paper presents a bio-inspired model for visual perception of motion through its principal indicator : the neuromimetic motion indicator (NMI). This indicator emerges out of the mechanism of antagonist interactions (MAI) where an architecture of oriented columns, local and distributed interactions of the neurons in the primary visual cortex (V1) is operated. The NMI indicator classifies the motion in : null motion and motion, and it estimates the number of moving objects in the scene.

## 1 Introduction

Several bio-inspired models exist for visual perception of motion. Some of them are inspired by the primary visual cortex (V1) with a strong neural cooperative-competitive interactions that converge to a local, distributed and oriented auto-organisation [1, 2, 3]. The others are inspired by the middle temporal area (MT) with the cooperative-competitive interactions between V1 and MT and an influence range [4, 5]. And some others are inspired by the middle superior area (MST) for the coherent motion and ego-motion [6, 7].

These models are based on the local detections by integration of various work directions upon different scales and spaces to end with a global answer. In this paper I present a neuromimetic approach for visual perception of motion that classifies the motion, first into two types : null motion and motion; next, it estimates the number of moving objects in the scene.

I will show the main characteristics of the main stage of the model proposed by [8] (MAI mechanism). Next, I manipulate its different parameters. Finally, I show the principle of my neuromimetic motion indicator and some results.

## 2 Neuromimetic connectionist architecture

This section present the main characteristics of the bio-inspired model for motion description based on the connectionist approach reported in [8, 9].

### 2.1 Causal spatio-temporal filtering (CSTF)

The first stage of this bio-inspired connectionist approach is mainly based on the causal spatio-temporal Gabor-like filtering and the second stage is a local and massively distributed processing.

---

\*This research was partially funded by project number 51623 from "Fondo Mixto Conacyt-Gobierno del Estado de Tamaulipas".

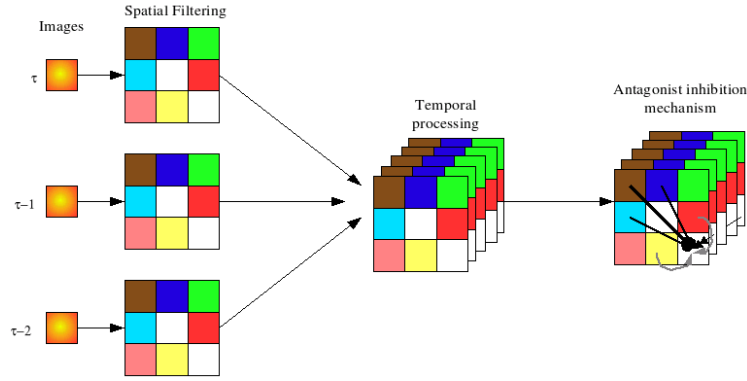


Fig. 1: Architecture of bio-inspired connectionist model (adapted of [9]).

This filtering is performed in two steps (see equation 1) : a Gabor-like spatial filtering and a causal temporal processing [10, 9].

$$H_{t,\theta,\vec{v}}(x, y) = \int S_{\theta}(x - \hat{v}_1, y - \hat{v}_2) dt \quad (1)$$

$$\hat{v}_1 = \frac{\hat{t}}{\tau - 1} v_1 \cos\theta, \quad \hat{v}_2 = \frac{\hat{t}}{\tau - 1} v_2 \sin\theta \quad (2)$$

where  $S_{\theta}(\cdot, \cdot)$  is the Gabor-like spatial filtering,  $\vec{v} = (v_1, v_2)$  the speed vector and  $\tau$  the number of images in the subsequence, and  $0 \leq \hat{t}, t < \tau$ .

For the spatial filtering, Gabor-like filters are implemented as image convolution kernels in  $\Theta$  different directions. I usually work with  $\Theta = 8$  for simplicity.

## 2.2 Mechanism of Antagonist Interactions (MAI)

The second stage of the model described in [8] (depicted to the right of figure 1) emulates a mechanism of antagonist interactions by means of excitatory-inhibitory local interactions in the different oriented cortical columns of V1.

Usually in excitatory-inhibitory neural models, the weighted connections to and from neurons have modulated strength according to the distance from one another. Nevertheless, I call it a mechanism of antagonist interactions because the inhibitory connections among neurons regulate downwards the activity of opposing or antagonist neurons, i.e. neurons that do not share a common or similar orientation and speed. On the other hand, excitatory connections increase the neuron activity towards the emergence of coherent responses, i.e. grouping neuron responses to similar orientations and speeds through an interactive process.

Then the updating of the internal state of a neuron is

$$\eta \frac{\partial H(x, y, T)}{\partial T} = -A \cdot H(x, y, T) + (B - H(x, y, T)) \cdot Exc(x, y, T) - (C + H(x, y, T)) \cdot Inh(x, y, T) \quad (3)$$

where  $-A \cdot H(\cdot)$  is the passive decay,  $(B - H(\cdot)) \cdot Exc(\cdot)$  the feedback excitation and,  $(C + H(\cdot)) \cdot Inh(\cdot)$  the feedback inhibition. Each feedback term includes a state-dependent nonlinear signal ( $Exc(x, y, T)$  and  $Inh(x, y, T)$ ) and an automatic gain control term ( $B - H(\cdot)$  and  $C + H(\cdot)$ , respectively).  $H(x, y, T)$  is the internal state of the neuron localised in  $(x, y)$  at time  $T$ ,  $Exc(x, y, T)$  is the activity due to the contribution of excitatory interactions in the neighbourhood  $\Omega_{(x,y)}^{\Omega_E}$  and  $Inh(x, y, T)$  is the activity due to the contribution of inhibitory interactions in the neighbourhood  $\Omega_{(x,y)}^{\Omega_I}$ . Both neighbourhoods depend on the activity level of the chosen neuron in each direction.  $A$ ,  $B$  and  $C$  are the real constant values and  $\eta$  is the learning rate. For more details on the excitation and inhibition areas see [8, 9].

Let  $\rho$  be the influence range of neuron  $(x, y)$  in this stage. This neuron receives at most  $\rho^2$  excitatory connections from neurons with the same direction and speed and at most  $(V \cdot \Theta - 1) \cdot \rho^2$  inhibitory connections from other close neurons.

At this level, each pixel correspond to  $\Theta \cdot V$  different neurons that encode informations of directions and speeds.

### 3 Neuromimetic motion indicator (NMI)

To obtain the NMI indicator, I generate a set of controlled sequences of real images and I make the relations between the different values of active neurons and their variations (§3.1). Next, I propose the basic ranges and their relations with the other sizes of images (§3.2).

#### 3.1 Behaviour of NMI in the controlled sequences of real images

The equation 3 shows the updating rule in the MAI for the neurons. Let  $S$  be a real image sequence and let  $R \subset S$  be a subsequence with  $Card(R) = \tau$  (the subsequence size) and let  $p$  be the percentage of the neurons to update.

The MAI mechanism updates  $p\%$  of active neurons (if  $H_{t,\theta,\vec{v}}(x, y) > 0.5$ ) and I obtain in it two frequencies : the active neurons after updating ( $ANaU$ , after application of the equation 3) and negative updating increase ( $NUI$ , only the frequency of  $(B - H(\cdot)) \cdot Exc(\cdot) - (C + H(\cdot)) \cdot Inh(\cdot) < 0$  in the equation 3).

The product between  $ANaU$  and  $NUI$  in all the different controlled subsequences inspire us to propose our neuromimetic indicator : *neuromimetic motion indicator*,  $NMI = ANaU * NUI$ .

In the table 1 I show the percentages of  $ANaU$ ,  $NUI$  and  $NMI$  for controlled sequences of real images with ego-motion. In almost all the cases  $NMI > 100.00$ . Only two cases showed inferior values due to very weak changes of contrasts got by my Gabor-like filters. But all values of  $NMI$  increase according to speed.

For motion classification, I took a subsequence of each sequence of real images : a) the motion does not exist and b) the motion exist. The table 2 shows the obtained values of sequences of real images (two first lines) and the well-known sequence of Yosemite Fly-Through.

	S	↑	↓	→	←	↙	↘	↖	↗
<i>ANaU</i>	1	34.80	30.23	28.98	22.73	27.66	30.23	36.60	40.72
	2	47.77	45.64	42.52	36.87	41.50	46.44	51.87	50.89
	3	50.12	47.87	44.81	39.55	42.33	42.82	48.16	50.40
<i>NUI</i>	1	4.75	3.88	2.93	1.96	3.69	3.89	4.82	7.79
	2	9.51	7.55	7.20	4.87	6.11	6.81	8.71	11.09
	3	11.73	9.92	8.75	5.95	7.05	8.00	9.87	11.57
<i>NMI</i>	1	165.32	117.27	84.80	44.55	102.02	117.68	176.35	317.06
	2	454.53	344.75	306.16	179.67	253.62	316.05	451.85	564.54
	3	587.99	474.98	392.15	235.26	298.45	342.70	475.20	583.11

Table 1: Percentages of frequencies of *NMI* behaviour for the controlled sequences of real images where there is ego-motion.

Sequence	Size	<i>ANaU</i>	<i>NUI</i>	<i>NMI</i>
Mist KW	442368	0.00	0.11	0.00
Walk	110594	0.14	0.13	0.02
Yosemite	79632	48.94	7.28	356.16

Table 2: Percentages of frequencies of *NMI* behaviour for the sequences-type.

The first sequence show the null motion; next, motion and, finally, ego-motion. But the different sizes of images influence the *NMI* values. The interpretation of the different values obtained are shown in the next subsection.

### 3.2 Motion type

According to the values shown in the tables 1 and 2, the *NMI* indicator discriminates the null motion and motion.

The table 3 shows the proposed ranges for *NMI* and their adaptation for the Kalsruhe-Wilhelm-Strasse. The basic ranges have been obtained for a sequence of real images of  $384 \times 288$  pixels (second column). The adaptation of different sizes of images follow this criterion :

$$Cond_{new} = \begin{cases} \left(1 - \frac{A_{new} * 100}{4A_{base}}\right) NMI_{base} & \text{if } A_{new} > A_{base} \\ \left(1 + \frac{A_{new} * 100}{4A_{base}}\right) NMI_{base} & \text{if } A_{new} < A_{base} \end{cases} \quad (4)$$

where  $A_{base}$  and  $A_{new}$  are the areas in pixels of the basic and new image, respectively.

## 4 Experiment results

The free parameters were set according to the suggestions in [8]. I present the results for the sequence Karl-Wilhelm-Strasse (KWS). This is a road traffic

Description	Basic ranges	KWS
Null motion	$NMI < 0.10$	$< 0.00$
Small objects or noise	$NMI < 1.00$	$< 0.01$
1 to 2 objects	$NMI < 5.00$	$< 0.05$
3 to 5 objects	$NMI < 10.00$	$< 0.10$
6 to 9 objects	$NMI < 40.00$	$< 0.40$
10 or more objects	$NMI < 145.00$	$< 1.45$

Table 3: Adaptation basic ranges of the neuromimetic motion indicator ( $NMI$ ).

sequence obtained by a surveillance camera and they are available in the Institute for Algorithm and Cognitive Systems of the Karlsruhe University, Germany (1541 images of  $768 \times 576$  pixels in RGB format).

The figure 2 shows four images of this sequence and the graph of its neuromimetic motion indicator ( $NMI$ ).

The KWS sequence shows the road traffic in normal conditions. The  $NMI$  for this sequence shows four moments of weak neural activities : the first two with one or two moving objects (images 153 to 190 and 549 to 596) and the last ones with a short instance with null motion (images 873 to 881 and 1534 to 1537).

Apart from these weak neural activities there are also three peaks in the  $NMI$  graph of KWS. The first one corresponds to tramway movement, the second one to movement of the cars and the last one to many moving cars. According to the table 3 there are 6 to 9 moving objects (and within them there are more than 10 at a moment), more than 10 moving objects, 6 to 9 moving objects and more than 10 moving objects, respectively.

The sudden changes in the  $NMI$  values owe to the sudden appearance or disappearance in general of a mobile object in the scene.

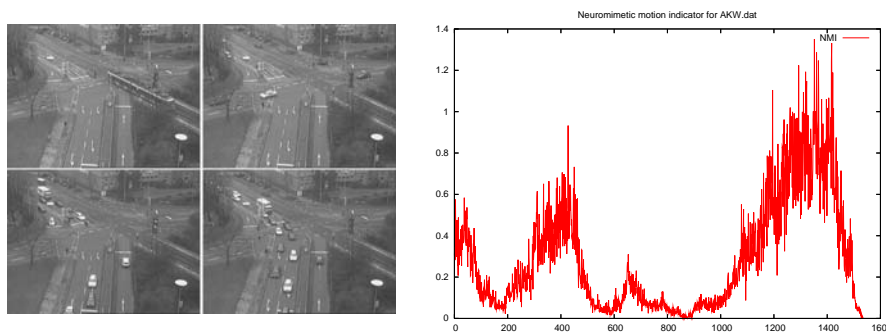


Fig. 2: From the top-left to the down-left in clockwise direction four images of the sequence. In the second column its neuromimetic motion indicator.

## 5 Conclusions

This work is based on the Castellanos model [9] : a neuromimetic connectionist model for visual perception of motion. A model fully inspired by the visual cortex system, the superior areas and their relations.

In this paper I took advantage of the low-level analysis to detect local motions to obtain the global indicator : the *neuromimetic motion indicator* issued by MAI mechanism.

My first experiments show that this model is capable to estimate the null motion, simple motion and an estimate of the number of moving objects. The estimation of motion is robust in quite complex scenes without any predefined information. Nevertheless, the estimation of *NMI* is fastidious. The experimental base values were verified for the sequences of real images of  $384 \times 288$  pixels and their adaptations for other sizes are proportional.

My current work includes experimenting on the influence of relative sizes of moving objects in the sequences, their contrasts and speeds and studying the same neuromimetic indicators for the moving fields only.

## References

- [1] Winfried A. Fellez and John G. Taylor. Establishing retinotopy by lateral-inhibition type homogeneous neural fields. *Neurocomputing*, 48:313–322, 2002.
- [2] Peter E. Latham and Sheila Nirenberg. Computing and stability in cortical networks. *Neural Computation*, pages 1385–1412, 2004.
- [3] Sorin Moga. *Apprendre par imitation: une nouvelle voie d'apprentissage pour les robots autonomes*. PhD thesis, Université de Cergy-Pontoise, Cergy-Pontoise, France, September 2000.
- [4] Eero P. Simoncelli and David J. Heeger. A model of neural responses in visual area mt. *Vision Research*, 38(5):743–761, 1998.
- [5] Ennio Mingolla. Neural models of motion integration and segmentation. *Neural Networks*, 16:939–945, 2003.
- [6] Christopher Pack, Stephen Grossberg, and Ennio Mingolla. A neural model of smooth pursuit control and motion perception by cortical area mst. Technical Report CAS/CNR-TR-99-023, Department of Cognitive and Neural Systems and Center for Adaptive Systems, 677 Beacon St, Boston, MA 02215, September 2000.
- [7] Richard S. Zemel and Terrence J. Sejnowski. A model for encoding multiple object motions and self-motion in area mst of primate visual cortex. *The Journal of Neurosciences*, 18(1):531–547, 1998.
- [8] Claudio Castellanos-Sánchez. *Neuromimetic connectionist model for embedded visual perception of motion*. PhD thesis, Université Henri Poincaré (Nancy I), Nancy, France, oct 2005. Bibliothèque des Sciences et Techniques.
- [9] Claudio Castellanos-Sánchez, Bernard Girau, and Frédéric Alexandre. A connectionist approach for visual perception of motion. In Leslie Smith, Amir Hussain, and Igor Aleksander, editors, *Brain Inspired Cognitive Systems (BICS 2004)*, pages BIS3-1:1–7, September 2004.
- [10] César Torres-Huitzil, Bernard Girau, and Claudio Castellanos-Sánchez. On-chip visual perception of motion: A bio-inspired connectionist model on fpga. *Neural Networks*, 18(5-6):557–565, June 2005.